Taylor & Francis
Taylor & Francis Group

View angle effects on the discrimination of selected Amazonian land cover types from a principal-component analysis of MISR spectra

ALEXANDRE SILVA XAVIER*† and LÊNIO SOARES GALVÃO‡

†Instituto de Estudos Avançados (IEAv), Rodovia dos Tamoios, km 5,5,
Torrão de Ouro, 12228-840, São José dos Campos, SP, Brazil
‡Instituto Nacional de Pesquisas Espaciais (INPE), Divisão de Sensoriamento Remoto,
Caixa Postal 515, 12245-970, São José dos Campos, SP, Brazil

Multi-angle Imaging Spectroradiometer (MISR) data, collected in four bands and at nine view angles in the Brazilian Amazon region, were used to describe view-angle effects on the spectral response and discrimination of three forest types; close and open lowland forests, open submontane forest and green/emerging pastures. A principal-component analysis (PCA) was applied over 450 bidirectional reflectance factor (BRF) MISR spectra (10 pixels, five land covers and nine view angles) to characterize the spectral-angular variability in the dataset and to identify the best view direction to enhance land cover discrimination. The analysis was extended into the images of the different cameras, which were classified for the presence of the forest covers using the minimum distance of the pixels to the average PC1 and PC2 scores of each forest class calculated from spectra analysis. Results showed an increase in the mean reflectance over the spectral bands (brightness) of the land covers from nadir to extreme viewing, as indicated by the first principal component, especially in the backward direction due to the predominance of sunlit view vegetation components. The transition from the backward (sunlit view surface components) to the forward (shaded view surface components) scattering directions was also characterized by changes in the shape of the BRF spectra, as indicated by decreasing PC2 score or near-infrared/blue ratio values. The variations in the MISR BRF followed the regularities expected from theory. PCA results also indicated that the best viewing to discriminate the forest types was the backward scattering direction ($-26.1°$ view angle), whereas the less favourable viewing was the forward scattering direction under the view shading condition (e.g. $+45.6°$ view angle). The overall classification accuracy for the three forest types increased from 52.4% at $+45.6°$ view angle to 78.7% at nadir, and to 95.0% at a $-26.1°$ view angle. From nadir to extreme view angles, directional effects produced a NDVI decrease for the forest types and an NDVI increase for the green and especially emerging pastures. Results demonstrated that data acquisition in off-nadir viewing may improve the discrimination and mapping of the Amazonian land cover types.

1. Introduction

To increase the spatial and temporal coverage of the remotely sensed areas and to improve the chance of selecting cloud-free data, large field-of-view (FOV)

---

*Corresponding author. Email: lenio@dsr.inpe.br

instruments are usually used in remote sensing applications (e.g. the Moderate Resolution Imaging Spectroradiometer (MODIS)). On the other hand, the off-nadir viewing introduces changes in sensor signal in response to variations in the geometry of data acquisition due to the non-Lambertian condition of the land cover types (Kimes *et al.* 1994, Leroy and Roujean 1994, Verbrugghe and Cierniewski 1995, Hu *et al.* 2000). The resulting directional effects are target- and wavelength-dependent and have been considered in the literature both as a source of noise and as a potential source of information for remote sensing applications (Kimes *et al.* 1984a, Roujean *et al.* 1992, Johnson 1994, Walthall 1997, Asner *et al.* 1998). Although empirical and physical approaches have been proposed to model such effects, a better knowledge of how sunlight is scattered in different directions by the land covers of the different environments is still necessary.

The Multi-angle Imaging Spectroradiometer (MISR) sensor on-board the Terra platform, launched in December 1999, acquires data in three visible and one near-infrared bands from nine view directions at a 1.1-km spatial resolution (Diner *et al.* 1998). Owing to recent advances in multi-angular imaging technology, MISR provides unique data to assess the anisotropy of the atmosphere and of the surface components, and to improve quantification of the vegetation photosynthetic activity and the structure of plant canopies (Martonchik *et al.* 1998, Gobron *et al.*, 2000, 2002). Thus, data collected in 36 channels (four bands and nine view angles), radiometrically calibrated and spatially coregistered, can be analysed on a per-pixel basis.

The objective of this investigation was to use MISR data collected in the Brazilian Amazon region to describe view angle effects on the spectral response and discrimination of selected land cover types. For this purpose, a principal-component analysis (PCA) was applied to bidirectional reflectance factor (BRF) spectra representative of the selected land cover types: (a) to reduce data dimensionality; (b) to identify the most important spectral intervals responsible for the variability in the directional reflectance; (c) to establish the spectral similarity between the land covers at different view angles; and (d) to indicate the best view direction to enhance land cover discrimination.

2. Methodology

The study area is located close to the limits of the states of Acre, Rondônia and Amazonas (Northwestern Brazil) between the geographic coordinates 68°00′ W, 8°40′ S (upper-left corner) and 65°00′ W, 10°00′ S (lower-right corner). It is characterized by the presence of primary tropical rainforest and by land cover types derived from its conversion such as pasture, crops and vegetation regrowth after land abandonment. The annual rainfall and mean temperature are of the order of 1900 mm and 24°C, respectively.

MISR data were obtained on 28 July 2000 at 1.1-km spatial resolution with the following nominal view angles relative to the Earth's surface: 70.5°, 60.0°, 45.6°, and 26.1° forward (cameras Af, Bf, Cf and Df) and aftward (cameras Aa, Ba, Ca and Da) of nadir, and 0° (nadir camera An). Each of the nine cameras acquired data, in 7 min at most, in four radiometrically calibrated, georectified and spatially coregistered spectral bands: blue (425–467 nm), green (543–572 nm), red (661–683 nm), and near-infrared (846–886 nm). A detailed description of the instrument can be found in Diner *et al.* (1998).

The following five land cover types were chosen in the investigation: tropical close ombrophilous lowland forest, tropical open ombrophilous lowland forest, tropical

open ombrophilous submontane forest, green pasture and emerging pasture. The aforementioned forest classes have a very important spatial distribution in the Amazon region. BRF spectra representative of these land cover types were selected from the nadir camera image by the comparison between isodata unsupervised classification results and available ground, and vegetation map information from previous studies (Fonseca *et al.* 1976, Silva *et al.* 1978, IBGE 1993, Sestini *et al.* 2002). Each land cover type was represented by 10 pixels with approximately similar positions at each camera image.

The analysis of MISR data consisted of the application of PCA, a common technique used in remote sensing and reflectance spectroscopy to facilitate the interpretation of a large number of spectra (Smith *et al.* 1985, Galvão *et al.* 1995, 1997, 2001, Palacios-Orueta and Ustin 1998). An example of the use of PCA, including the equations used to obtain the eigenvalues, eigenvectors and the PC scores can be found in Davis (1986). In the present study, PCA was applied over 450 MISR spectra (10 pixels, five land cover types and nine view angles) using the BRF values of its four bands as input variables. A correlation matrix, derived from the reflectance values of the four MISR bands, provided the basis for the eigenvalue and eigenvector calculations and for the subsequent determination of the PC scores. Each score represents a transformed spectrum from the linear combination of the reflectance of the bands. By analysing the eigenvectors and the PC score differences, the contribution of each band for the variability in the dataset and the spectral similarity between the land covers at each view angle could be established, respectively. View angle effects on the normalized difference vegetation index (NDVI=(near-infrared – red)/(near-infrared + red)) were also analysed.

Finally, to analyse the results of the previous PC analysis of MISR spectra on a per-pixel basis, a mask was created in the MISR image using available maps as references (IBGE 1993, Sestini *et al.* 2002) to represent major areas of occurrence of the three forest types. By using the factor score coefficient matrix, derived from PCA of MISR spectra, the PC scores were computed on a per-pixel basis for each camera. By calculating the Euclidean distance of these scores to the group centroids (average PC scores of each group determined from spectra analysis), the pixels were classified for the presence of the three forest classes. The mask map image was then compared with the PC-derived mask classified image at the different cameras to indicate the best view direction to enhance forest cover discrimination.

3. Results and discussion

3.1 *MISR imagery and land cover types*

Figure 1(*a*) illustrates the geometry of MISR data acquisition. MISR collected data with solar azimuth and zenith angles of $217 \pm 1.42°$ and $36 \pm 0.63°$, respectively, and the following actual view zenith angles: $70.3 \pm 0.07°$, $60.0 \pm 0.08°$, $45.5 \pm 0.11°$, and $26.1 \pm 0.16°$ (cameras Af, Bf, Cf and Df), $2.4 \pm 1.37°$ (nadir) and $26.3 \pm 0.21°$, $45.8 \pm 0.12°$, $60.2 \pm 0.08°$, $70.4 \pm 0.07°$ (cameras Aa, Ba, Ca and Da). In this study, negative (cameras forward) and positive (cameras aftward) view angles indicate the backward and forward scattering directions, respectively (figure 1(*a*)).

Figure 1(*b*) shows a schematic representation of the biomass decrease in the study area from the close lowland forest to the open submontane forest. From the 500 m MODIS vegetation continuous field dataset (Hansen *et al.* 2003), the following
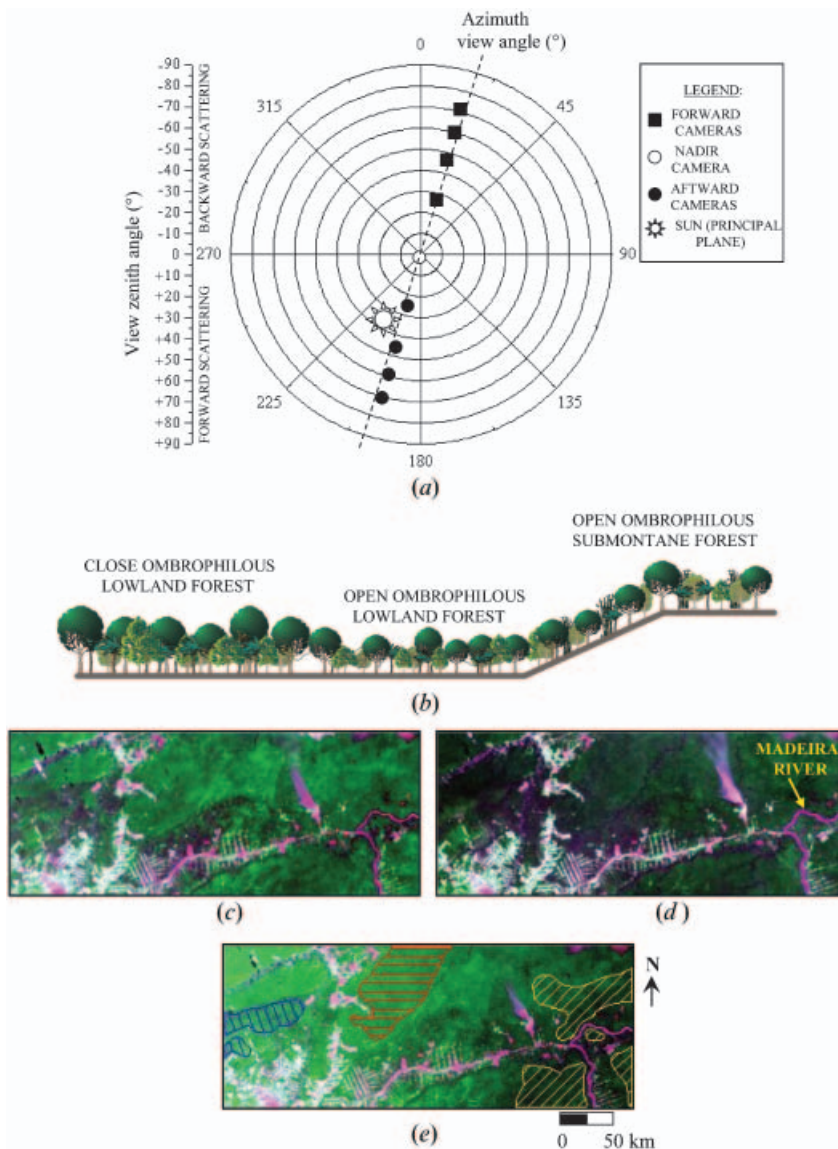
Figure 1. (*a*) Geometry of MISR data acquisition. (*b*) Schematic profile diagrams of the three studied forest types. In (*c*), (*d*) and (*e*), MISR color composites (bands 3 (red), 4 (green) and 2 (blue)) are shown for the backward (−70.5°) and forward (+60.0°) scattering directions, and for the nadir (0°), respectively. Areas representative of close (red polygon) and open (blue polygons) lowland forests, and open submontane forest (yellow polygons) are indicated in (*e*).

average tree covers were obtained: 87.3%±4.5 (close lowland forest), 83.1%±4.4 (open lowland forest), and 81.2%±4.8 (open submontane forest).

Examples of MISR colour composites (bands 3 in red, 4 in green, and 2 in blue) for data collected at large view angles (figures 1(*c*) and 1(*d*)) and at nadir (figure 1(*e*)) are also presented. Portions of the scene representative of the three forest types, selected for investigation from the inspection of unsupervised classification results and available ground and map information, are indicated by polygons in figure 1(*e*).

The close lowland forest (red polygon), with emerging trees, predominates in the central portion of the scene, whereas the open lowland forest (blue polygons), with liana, palm trees and bamboo, occurs in the left side of the scene. The main occurrence of open submontane forest (yellow polygons), with palm trees and liana, is verified close to the Madeira River. Some small areas of emerging (magenta colour in figure 1(*e*)) and green (light green colour) pastures were selected along the entire scene to represent these land covers.

Thus, as a result of the Sun-viewing geometry illustrated in figure 1(*a*), the sensor detected more sunlit upper layer canopy components in the backward direction (e.g. bright image of figure 1(*c*)) than in the forward direction (e.g. dark image of figure 1(*d*)), in which a greater proportion of shaded lower layer canopy components was viewed. A discussion on the physical mechanisms responsible for the directional behaviour of canopies can be found in Kimes *et al.* (1984b).

3.2 *Spectral-angular reflectance variations from PCA*

Figures 2(*a*) and 2(*b*) show average BRF spectra calculated from 10 pixels for close lowland forest and open submontane forest, respectively. To facilitate graphic representation, results were presented only for five of the nine MISR cameras. In both figures, the cameras Bf and Df presented spectra with a higher reflectance than that observed in the cameras Ba and Da due to the prevalence of sunlit view canopy components in the backward scattering direction. When the sensor moved away from the backward direction, the reflectance decreased because of the increase in the relative proportion of the shadowed view canopy components. At nadir, in comparison with the close lowland forest, the open submontane forest showed a reflectance decrease in the near-infrared interval due to lower amounts of biomass and to differences in canopy architecture introduced by palm trees and liana.

A better understanding of the spectral-angular variations associated with the selected land covers was obtained from the inspection of the PCA results. Table 1 shows the resultant eigenvectors for the first two components derived from the use of PCA over 450 BRF spectra, using the reflectance values of the four MISR bands as input variables. The eigenvector values provide the contribution of each band to explain a given component. The first two principal components (PC1 and PC2) were responsible by 92.3% of the variance in the dataset. PC1, which accounted for 72.9% of the variance, represented the mean reflectance over the spectral bands (brightness), as indicated by the approximately similar positive eigenvector values (table 1). PC2, which accounted for 19.4% of the variance, expressed the spectral-angular variation associated with the near-infrared (band 4) and blue (band 1) bands, as indicated by the large positive and negative eigenvector values, respectively (table 1). Thus, PC2 indicated changes in the shape of the spectra due to viewing geometry that could be expressed by the near-infrared/blue reflectance ratio (MISR 4 : 1 ratio). Since the blue and red bands are usually highly correlated over vegetation, PC2 is also an indirect indicator of variations in vegetation indices such as the simple ratio (near-infrared/red) or even NDVI.

The projection of the average 45 scores (average of 10 pixels for five land cover types and nine view angles) along the first two principal-component axes (PC1 and PC2) is displayed in figure 3. Open and close symbols linked by a single line indicate spectra of a given land cover collected in the backward (Cameras 'f') and forward (Cameras 'a') scattering directions, respectively. The five PC curves of figure 3 could be divided into two general groups of angular response: forest and pasture classes.
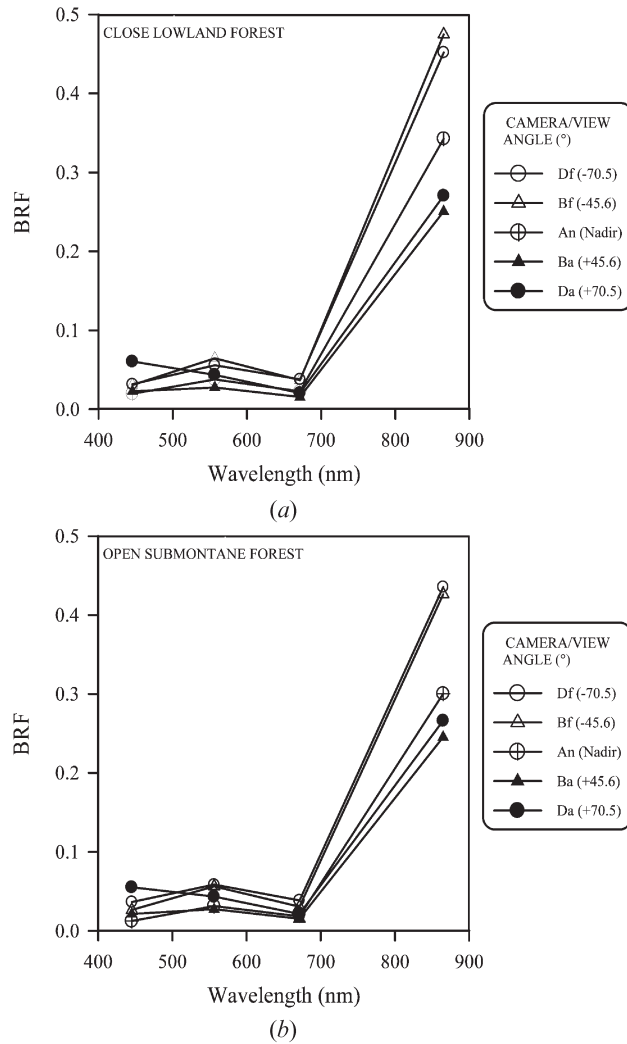
Figure 2.   Bidirectional reflectance factor (BRF) spectra (average of 10 pixels) collected at different MISR cameras over (*a*) the close lowland forest and (*b*) the open submontane forest.

The PC curves for the forest classes have approximately the same shape in the PC space. The same was verified between the green and emerging pasture curves. These results are in agreement with the discussion presented by Zhang *et al.* (2002) on the similarity of the angular signatures of 10 land covers and their subsequent aggregation into fewer biome types with distinct signatures.

Table 1. Eigenvector values for the first and second principal components.

	PC1	PC2
Band 1	0.267	−0.688
Band 2	0.339	0.033
Band 3	0.316	−0.122
Band 4	0.236	0.893
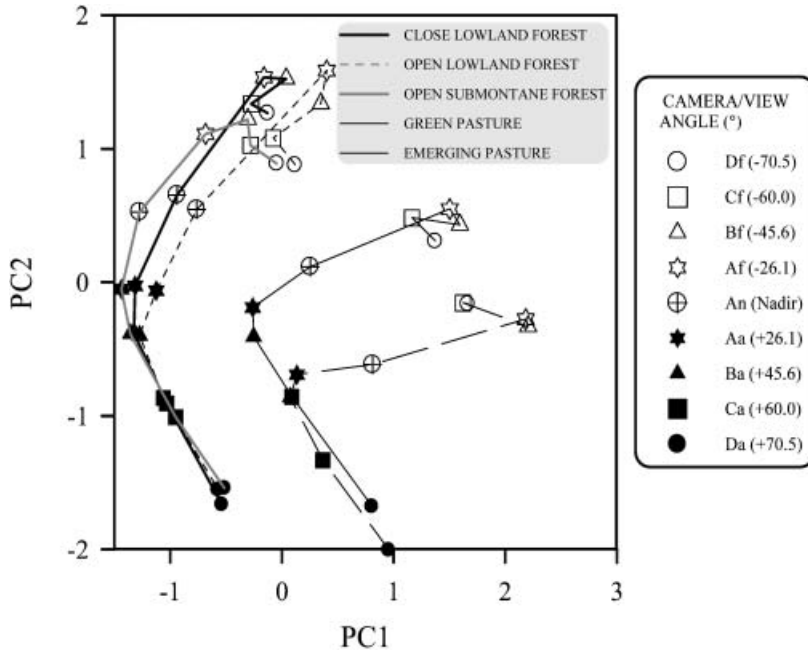
Figure 3. PC1 and PC2 scores (average of 10 pixels) as a function of nine view angles and five land cover types. Open and close symbols indicate the backward and forward scattering directions, respectively.

In figure 3, the mean reflectance over the spectral bands (brightness) tends to increase from the left to the right side of the PC1 axis, whereas the near-infrared/blue reflectance ratio tends to increase from the bottom to the top of the PC2 axis. Thus, as also indicated in figure 4(*a*), the mean reflectance tends to increase from the forest classes (low PC1 scores in figure 3) to the green and emerging pastures (high PC1 scores in figure 3), and from nadir to extreme viewing for all land covers. The increase in brightness occurred especially in the backward scattering direction (open symbols in figure 3) due to the predominance of sunlit view vegetation components. At nadir, the open submontane forest presented a lower mean reflectance than the other forest types. In figure 4(*a*), as indicated by the standard deviation bars, the spectral variability increased for a given camera from the forest classes to the green and emerging pastures. Among the forest classes, the two open forests presented larger standard deviation values than the close lowland forest. In general, the spectral variability of the mean reflectance increased from nadir to extreme view angles for all land covers.

The transition from the backward (sunlit view surface components) to the forward (shaded view surface components) scattering directions was also characterized by the displacement of the scores from the top to the bottom of the PC2 axis (figure 3). In figure 4(*b*), as expected, such displacement was equivalent to a decreasing near-infrared/blue reflectance ratio towards positive view angles, mostly as a result of shadowing in the forward scattering direction, especially due to the near-infrared band reflectance decrease. In comparison with the other forest classes, the open submontane forest showed the largest standard deviation values in figure 4(*b*).
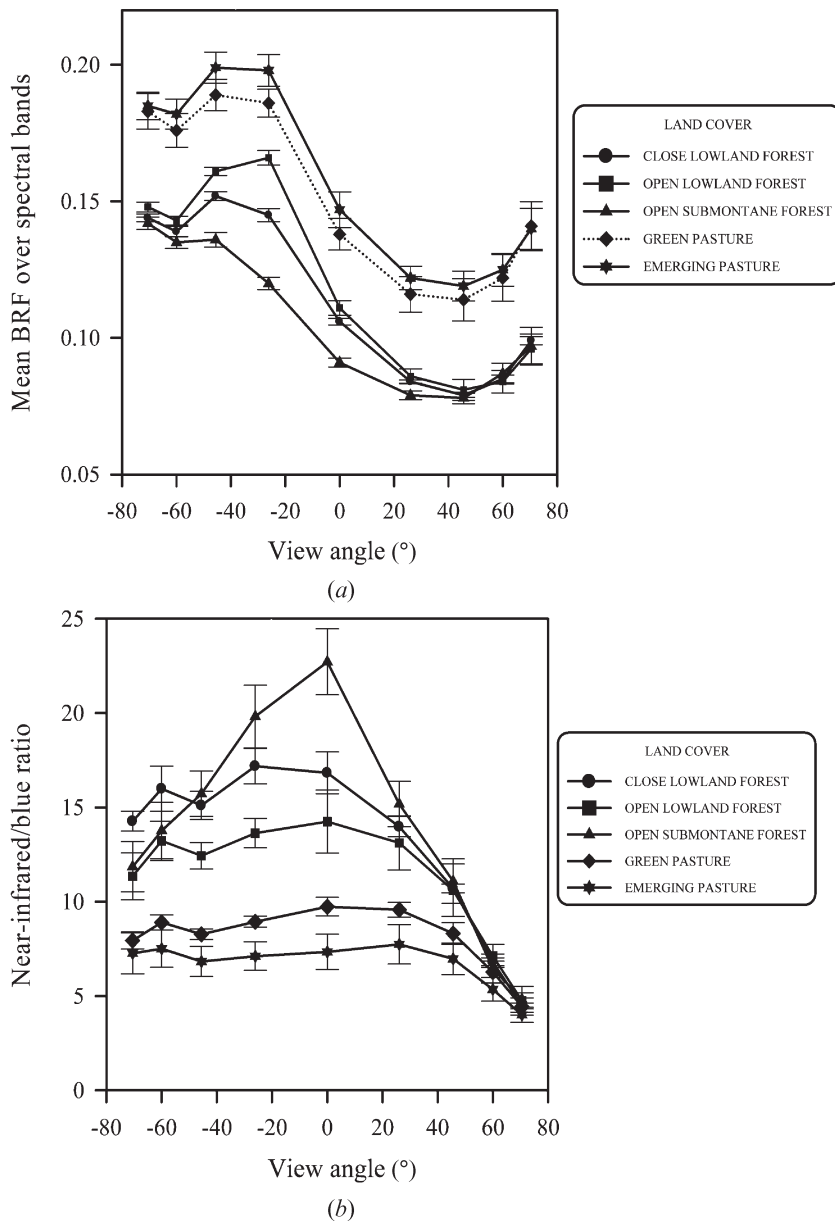
Figure 4. Angular variations (average of 10 pixels) for the five studied land cover types of the (*a*) mean bidirectional reflectance factor (BRF) over the spectral bands and (*b*) near-infrared/blue reflectance ratio values. Standard deviation bars are indicated.

To demonstrate the anisotropic spectral behaviour of the two general groups of land covers (forest and pasture), figure 5 shows average angular BRF profiles, normalized (ratioed) to the nadir response, for the open lowland forest and for the emerging pasture. In general, the forest types showed stronger variations due to view angles than the emerging and green pastures, as indicated by the wider range of the normalized BRF values observed for forests. For example, differences in the red band response relative to nadir were as high as +70%/−35% for the open lowland
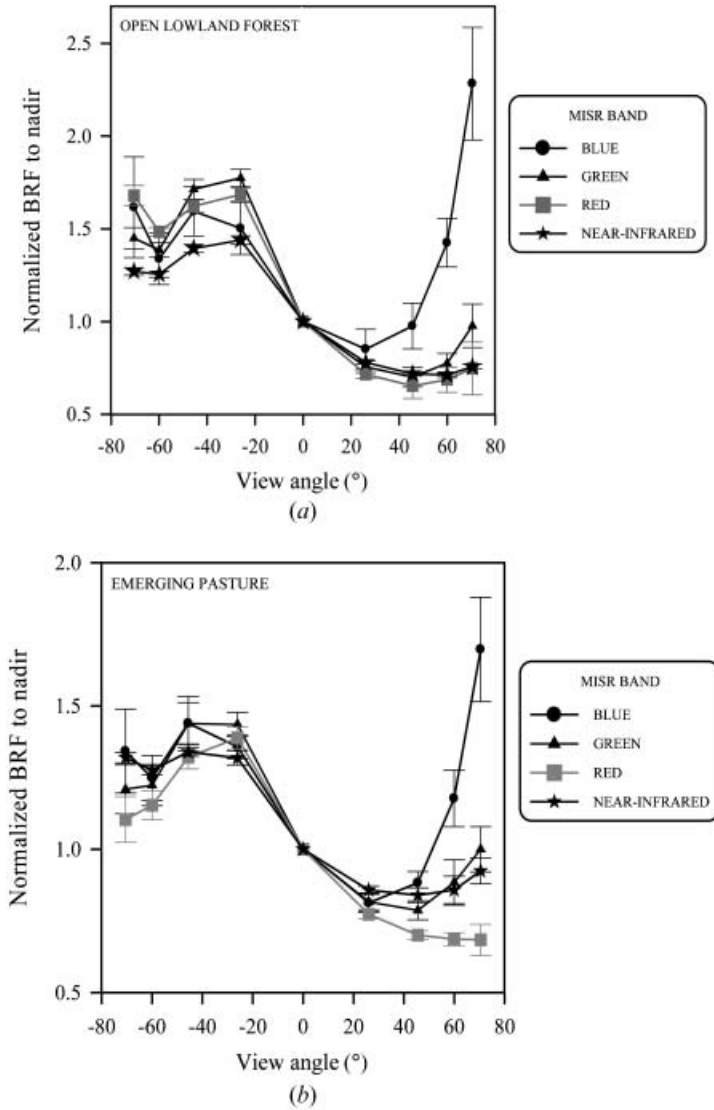
Figure 5. Bidirectional reflectance factor (BRF) angular profiles (average of 10 pixels) normalized to nadir for the (*a*) open lowland forest and (*b*) emerging pasture. Standard deviation bars are indicated.

forest (figure 5(*a*)) and $+30\%/-30\%$ for the emerging pasture (figure 5(*b*)) in the backward/forward directions, respectively. For the studied land covers, the minimum and maximum reflectance values of the red and near-infrared bands were observed in the forward ($+45.6°$ view angle) and backward scattering directions ($-26.1°$ and $-45.6°$ view angles), respectively. Similar trends have been reported for crops and grasses (Deering *et al.* 1992, Epiphanio and Huete 1995). According to Walter-Shea *et al.* (1997), the view angles at which minimum and maximum reflectance values are observed may vary with the solar zenith angle and leaf area index.
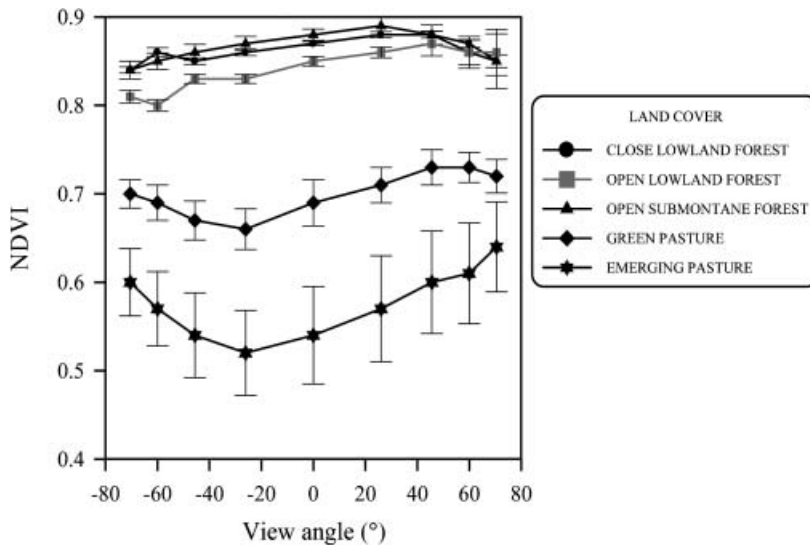
Figure 6. NDVI variations (average of 10 pixels) as a function of view angles for the studied land cover types.

The directional effects were not completely removed after the determination of NDVI (figure 6). NDVI variations with view geometry were stronger for emerging pasture than for green pasture, and decreased for the forest classes. In relation to the nadir response, NDVI differences increased at extreme viewing from 0.05 for the forest classes to 0.10 for emerging pasture. In general, NDVI decreased from nadir to extreme view angles for the forest types due to the relatively stronger increase in their red response than in their near-infrared reflectance, especially in the backward scattering direction (figure 5(*a*)). On the other hand, NDVI values increased towards extreme viewing for emerging pasture due to the relative increase in its near-infrared response and to the relative decrease in its red reflectance in both scattering directions (figure 5(*b*)). These results are in agreement with previous investigations that demonstrated that NDVI variations with Sun-view geometry are stronger as the leaf area index decreases (Walter-Shea *et al.* 1997, Kaufmann *et al.* 2000) and are dependent on the vegetation type (e.g. Jackson *et al.* 1990, Epiphanio and Huete 1995, Qi *et al.* 1995).

The magnitude of the NDVI variations due to view geometry (figure 6) may be affected to some extent by the uncertainties in MISR BRF data. The causes of these uncertainties were discussed by Hu *et al.* (2003). For example, in figure 6, NDVI uncertainties for the forest classes increased from nadir to extreme viewing, as indicated by larger standard deviation values observed with increasing view angles, especially in the forward scattering direction. Such uncertainties may result from the difficulties to remove scattering atmospheric effects on the red band at large view angles. On the other hand, green and emerging pastures presented generally similar standard deviation values at all view angles with slightly higher values near nadir.

3.3 Land covers discrimination from PCA

In the PC space of figure 3, small differences between the scores indicate spectral similarity between the land covers. The dispersion of the PC scores for the forest

types was greater in the backward direction (open symbols) than in the forward direction (close symbols), which suggested better possibilities of spectral discrimination in the backward direction. On the other hand, the less favourable direction for forest cover discrimination occurred at +45.6° (shadowing direction), as expressed by the proximity of the PC scores in figure 3 (closed triangles).

To indicate the best view direction to enhance forest discrimination, PC score differences between the close and open lowland forests ($PC_{close-forest}$ minus $PC_{open-forest}$) were plotted as a function of view angles (figure 7). At a given direction, small PC score differences indicate spectral similarity between the two land covers, whereas large differences indicate dissimilarity. The best direction for the discrimination of the two forest types was verified at the −26.1° view angle (backward direction) that exhibited the greatest PC1 and PC2 score differences. On the other hand, the less favourable viewing was the forward scattering direction under view shading condition (e.g. +45.6° view angle).

To confirm the results of figure 7 on a per-pixel basis, figure 8(*a*) shows areas of major occurrence of the three forest types extracted from available maps (IBGE 1993, Sestini *et al.* 2002). Figures 8(*b*), 8(*c*) and 8(*d*) illustrate the classification results for mask images from the cameras Ba (+45.6°), An (nadir) and Af (−26.1°), respectively. The criterion used for classification was the minimum distance of the pixels of the first two PC images to the average PC1 and PC2 scores (group centroids) calculated from the previous PCA of BRF spectra. In the forward scattering direction (figure 8(*b*)), the three forest types were not adequately discriminated. At nadir (figure 8(*c*)), the open submontane forest was correctly discriminated, but several pixels of the close and open lowland forests were misclassified. Finally, in the backward scattering direction (−26.1° view angle), the three forest types were adequately discriminated (figure 8(*d*)). The overall classification accuracy increased from 52.4% (+45.6° view angle) to 78.7% (nadir), and to 95.0% (−26.1° view angle). In figure 9, the classification accuracy for the close and open lowland forests increased from 70% at nadir to 95% at a −26.1° view angle.
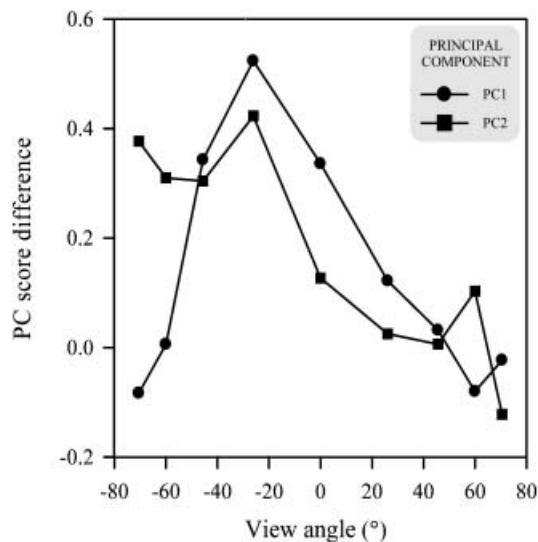
Figure 7. Differences in the average PC1 and PC2 scores as a function of view angles between the close and open lowland forests. Large score differences indicate dissimilarity.
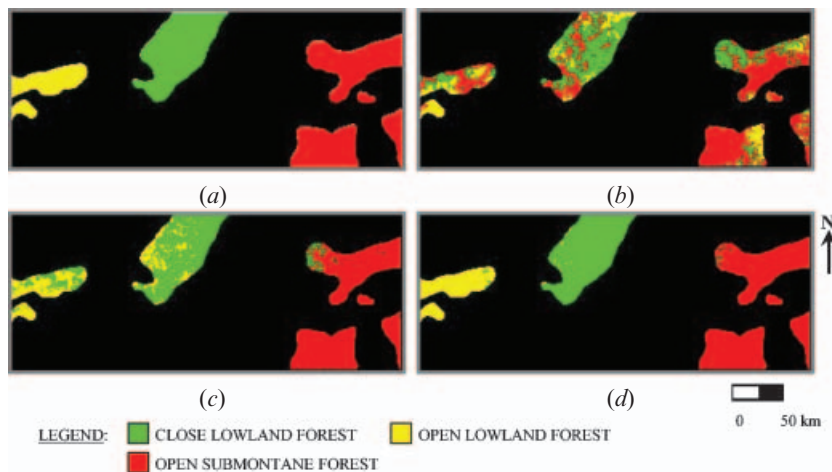
Figure 8. (*a*) Areas of major occurrence of the three forest types. The minimum distance classification results for the mask images from the cameras Ba (+45.6°), An (nadir) and Af (−26.1°) are presented in (*b*), (*c*) and (*d*), respectively. The first two principal-component images and the corresponding average PC1 and PC2 scores, calculated from PCA of BRF spectra, were used in the classification.

4. Conclusions

Directional effects produced an increase in the mean reflectance over the spectral bands from nadir to extreme viewing, especially in the backward direction due to the predominance of sunlit view vegetation components. In general, variations in MISR BRF followed regularities expected from theory. The mean reflectance over the spectral bands (brightness), represented by the PC1 values, increased from the forest types to the green and emerging pastures. It also increased from the open submontane forest to the open lowland forest at nadir. However, such a relationship between the forest types changed with increasing view angles in both scattering
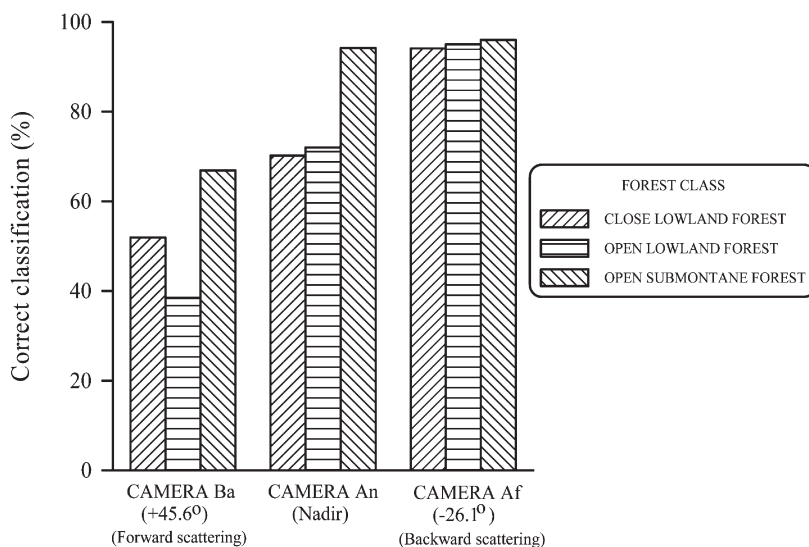
Figure 9. Classification accuracy for the three forest types and three view angles.

directions, which demonstrated the target dependence of the directional effects in the Brazilian tropical rainforest. The transition from the backward (sunlit view surface components) to the forward (shaded view surface components) scattering directions was also characterized by changes in the shape of the spectra. These changes were expressed by decreasing near-infrared/blue ratio values or PC2 scores, mostly as a result of shadowing in the forward scattering direction. Directional effects also affected the NDVI determination of the selected land cover types producing an NDVI decrease for the forest types and an NDVI increase for the green and emerging pastures from nadir to extreme view angles.

PCA results indicated that the best viewing to discriminate the forest types was the backward scattering direction. The greatest dissimilarity between the three forest types was verified at the $-26.1°$ view angle, as indicated by the largest PC1 and PC2 score differences. On the other hand, the greatest similarity occurred in the forward scattering direction (e.g. $+45.6°$ view angle) under the view shading condition. The overall classification accuracy of the three forest classes increased from 52.4% ($+45.6°$ view angle) to 78.7% (nadir), and to 95.0% ($-26.1°$ view angle). The classification accuracy for the close and open lowland forests increased from 70% at nadir to 95% at a $-26.1°$ view angle. The results demonstrated that data acquisition in off-nadir viewing may improve the discrimination and mapping of the Amazonian land cover types. These data were obtained from NASA langley Research Center Atmospheric Sciences Data Center.

References

ASNER, G.P., BRASWELL, B.H., SCHIMEL, D.S. and WESSMAN, C.A., 1998, Ecological research needs from multiangle remote sensing data. *Remote Sensing of Environment*, **63**, pp. 155–165.

DAVIS, J.C., 1986, *Statistics and Data Analysis in Geology* ((New York: Wiley).

DEERING, D.W., MIDDLETON, E.M., IRONS, J.R., BLAD, B.L., WALTER-SHEA, E.A., HAYS, C.J., WALTHALL, C., ECK, T.F., AHMAD, S.P. and BANERJEE, B.P., 1992, Prairie grassland bidirectional reflectances measured by different instruments at the FIFE site. *Journal of Geophysical Research*, **97**, pp. 18 887–18 903.

DINER, D.J., BECKERT, J.C., REILLY, T.H., BRUEGGE, C.J., CONEL, J.E., KAHN, R.A., MARTONCHIK, J.V., ACKERMAN, T.P., DAVIES, R., GERSTL, S.A.W., GORDON, H.R., MULLER, J., MYNENI, R.B., SELLERS, P.J., PINTY, B. and VERSTRAETE, M.M., 1998, Multi-angle Imaging SpectroRadiometer (MISR) instrument description and experiment overview. *IEEE Transactions on Geoscience and Remote Sensing*, **36**, pp. 1072–1087.

EPIPHANIO, J.C.N. and HUETE, A.R., 1995, Dependence of NDVI and SAVI on Sun/sensor geometry and its effect on FAPAR relationships in alfalfa. *Remote Sensing of Environment*, **51**, pp. 351–360.

FONSECA, W.N., KOURY, O., RIBEIRO, A.G., SILVA, S.B., FERREIRA, H.C., FONSECA, W.N. and RIBEIRO, A.G., 1976, Folha SC.19 Rio Branco: as regiões fitoecológicas, sua natureza e seus recursos econômicos. In *Projeto RadamBrasil,* Departamento Nacional da Produção Mineral (Eds), pp. 313–392 ((Rio de Janeiro: DNPM).

GALVÃO, L.S., VITORELLO, I. and PARADELLA, W.R., 1995, Spectroradiometric discrimination of laterites with principal components analysis and additive modelling. *Remote Sensing of Environment*, **53**, pp. 70–75.

GALVÃO, L.S., VITORELLO, I. and FORMAGGIO, A.R., 1997, Relationships of spectral reflectance and color among surface and subsurface horizons of tropical soil profiles. *Remote Sensing of Environment*, **61**, pp. 24–33.

GALVÃO, L.S., PIZARRO, M.A. and EPIPHANIO, J.C.N., 2001, Variations in reflectance of tropical soils: spectral–chemical composition relationships from AVIRIS data. *Remote Sensing of Environment*, **75**, pp. 245–255.

GOBRON, N., PINTY, B., VERSTRAETE, M.M., MARTONCHIK, J.V., KNYAZIKHIN, Y. and DINER, D.J., 2000, Potential of multiangular spectral measurements to characterize land surfaces: conceptual approach and exploratory application. *Journal of Geophysical Research*, **105**, pp. 17539–17549.

GOBRON, N., PINTY, B., VERSTRAETE, M.M., WIDLOWSKI, J. and DINER, D.J., 2002, Uniqueness of multiangular measurements—Part II: Joint retrieval of vegetation structure and photosynthetic activity from MISR. *IEEE Transactions on Geoscience and Remote Sensing*, **40**, pp. 1574–1592.

HANSEN, M., DEFRIES, R., TOWNSHEND, J.R., CARROLL, M., DIMICELI, C. and SOHLBERG, R., 2003, *500 m MODIS Vegetation Continuous Field* (College Park, MD: The Global Land Cover Facility).

HU, B., LUCHT, W., STRAHLER, A.H., SCHAAF, C.B. and SMITH, M., 2000, Surface albedos and angle-corrected NDVI from AVHRR observations of South America. *Remote Sensing of Environment*, **71**, pp. 119–132.

HU, J.N., TAN, B., SHABANOV, N., CREAN, K.A., MARTONCHIK, J.V., DINER, D.J., KNYAZIKHIN, Y. and MYNENI, R.B., 2003, Performance of the MISR LAI and FPAR algorithm: a case study in Africa. *Remote Sensing of Environment*, **88**, pp. 324–340.

INSTITUTO BRASILEIRO DE GEOGRAFIA E ESTATÍSTICA (IBGE) 1993, *Mapa de vegetação do Brasil. Map 1 : 5.000.000* ((Rio de Janeiro: IBGE).

JACKSON, R.D., TEILLET, P.M., SLATER, P.N., FEDOSEJEVS, G., JASINSKI, M.F., AASE, J.K. and MORAN, M.S., 1990, Bidirectional measurements of surface reflectance for view angle corrections of oblique imagery. *Remote Sensing of Environment*, **32**, pp. 189–202.

JOHNSON, L.F., 1994, Multiple view zenith angle observations of reflectance from Ponderosa pine stands. *International Journal of Remote Sensing*, **15**, pp. 3859–3865.

KAUFMANN, R.K., ZHOU, L., KNYAZIKHIN, Y., SHABANOV, N.V., MYNENI, R.B. and TUCKER, C.J., 2000, Effect of orbital drift and sensor changes on the time series of AVHRR vegetation index data. *IEEE Transactions on Geoscience and Remote Sensing*, **38**, pp. 2584–2597.

KIMES, D.S., HARRISON, P.A. and HARRISON, P.R., 1994, Extension of off-nadir view angles for directional sensor systems. *Remote Sensing of Environment*, **50**, pp. 201–211.

KIMES, D.S., HOLBEN, B.N., TUCKER, C.J. and NEWCOMB, W.W., 1984a, Optimal directional view angles for remote-sensing missions. *International Journal of Remote Sensing*, **5**, pp. 887–908.

KIMES, D.S., NEWCOMB, W.W., SCHUTT, J.B., PINTER, P.J. and JACKSON, R.D., 1984b, Directional reflectance factor distributions of a cotton row crop. *International Journal of Remote Sensing*, **5**, pp. 263–277.

LEROY, M. and ROUJEAN, J., 1994, Sun and view angle corrections on reflectances derived from NOAA/AVHRR data. *IEEE Transactions on Geoscience and Remote Sensing*, **32**, pp. 684–697.

MARTONCHIK, J.V., DINER, D.J., PINTY, B., VERSTRAETE, M.M., MYNENI, R.B., KNYAZIKHIN, Y. and GORDON, H.R., 1998, Determination of land and ocean reflective, radiative, and biophysical properties using multiangle imaging. *IEEE Transactions on Geoscience and Remote Sensing*, **36**, pp. 1266–1281.

PALACIOS-ORUETA, A. and USTIN, S.L., 1998, Remote sensing of soil properties in the Santa Monica Mountains. I. Spectral analysis. *Remote Sensing of Environment*, **65**, pp. 170–183.

QI, J., MORAN, M.S., CABOT, F. and DEDIEU, G., 1995, Normalization of Sun/view angle effects using spectral albedo-based vegetation indices. *Remote Sensing of Environment*, **52**, pp. 207–217.

ROUJEAN, J.L., LEROY, M. and DESCHAMPS, P.Y., 1992, A bidirectional reflectance model of the Earth's surface for the correction of remote sensing data. *Journal of Geophysical Research*, **97**, pp. 20455–20468.

SESTINI, M.F., ALVALA, R.C.S., MELLO, E.M.K., VALERIANO, D.M., REIMER, E.S., CHAN, S.C. and NOBRE, C.A., 2002, *Integração e atualização de dados de uso/cobertura do terreno da Amazônia Legal para utilização em modelos de superfície (SSiB)*, Technical Report 8972-RPQ/730, Instituto Nacional de Pesquisas Espaciais (INPE), São José dos Campos, SP, Brazil.

SILVA, S.B., SILVA, M.T.M., SILVA, F.C.F., COSTA, E.P., RIBEIRO, A.G. and FERREIRA, H.C., 1978, Folha SC.20 Porto Velho: as regiões fitoecológicas, sua natureza e seus recursos econômicos. In *Projeto RadamBrasil,* Departamento Nacional da Produção Mineral (Eds), pp. 413–562 ((Rio de Janeiro: DNPM).

SMITH, M.O., JOHNSON, P.E. and ADAMS, J.B., 1985, Quantitative determination of mineral types and abundances from reflectance spectra using principal components analysis. *Journal of Geophysical Research*, **90**, pp. 797–804.

VERBRUGGHE, M. and CIERNIEWSKI, J., 1995, Effects of sun and view geometries on cotton bidirectional reflectance. Test of a geometrical model. *Remote Sensing of Environment*, **54**, pp. 189–197.

WALTHALL, C.L., 1997, A study of reflectance anisotropy and canopy structure using a simple empirical model. *Remote Sensing of Environment*, **61**, pp. 118–128.

WALTER-SHEA, E.A., PRIVETTE, J., CORNELL, D., MESARCH, M.A. and HAYS, C.J., 1997, Relations between directional spectral vegetation indices and leaf area and absorbed radiation in alfalfa. *Remote Sensing of Environment*, **61**, pp. 162–177.

ZHANG, Y., TIAN, Y., MYNENI, R.B., KNYAZIKHIN, Y. and WOODCOCK, C.E., 2002, Assessing the information content of multiangle satellite data for mapping biomes. *Remote Sensing of Environment*, **80**, pp. 418–434.